



Energy Flow Management and Size Optimization for Photo-Voltaic and Wind Renewable Sources Integrated with Vehicle-to-Grid Technology

*Mohamed Nuri Hussin, Mohamed Abdolla Hossin, Sadam Alnaghoughi

Renewable Energy Department, Faculty of Engineering, Sebha University, Libya

Keywords:

Energy flow management optimization
Vehicle-to-grid V2G
Renewable energy sources RESs
Search algorithms CSA & PSO.

ABSTRACT

The energy management process can increase the reliability of the energy flow to cover the load in a Hybrid Renewable Energy System (HRES), especially in light of the development of new technologies such as Vehicle-to-Grid (V2G) technology that helps the grid handle with peak load coverage. This paper deals with a connected hybrid system With the grid is used to operate a residential building in the Sabha region in southern Libya, as it consists of photovoltaic (PV) with a capacity of (112.8) KW, wind turbines (WT) generating (24) KW, batteries (BT) up to (63) KW, and electric vehicles (67) KW, with an investment of (513,432) thousand dollars. The proposed system generates (2338) Mw/h/year, which is sufficient to meet (54.76) % of the demand for electricity from renewable energy sources. It also generates surplus energy at a value of (0.91) Mw/h/year, meaning that the deficit in meeting energy demand is negligible. The system is designed to reduce the Levelized Cost of Energy (LCOE) and Loss of Power Supply Probability (LPSP) while increasing the Renewable Energy Fraction (REF) by implementing an energy management optimization strategy through search algorithms such as the Cuckoo search algorithm (CSA) and Particle swarm optimization (PSO) for component size. Hybrid renewable energy system, taking into account climatic data as well as objective functions and Constraints. The energy balance between system components is analyzed to obtain the best performance at the lowest operating cost. The system was set up using MATLAB codes in different configurations, and the obtained results show better performance values such as (0.0340) \$/KWh, (0.0769)%, and (0.5476)% for COE, LPSP, and REF, respectively.

إدارة تدفق الطاقة وتحسين الحجم لمصادر الطاقة المتجددة الكهروضوئية وطاقة الرياح المدمجة مع تكنولوجيا المركبة إلى الشبكة

*محمد نوري حسين و محمد عبدالله حسين و صدام النغونغي

قسم الطاقات المتجددة ، كلية الهندسة ، جامعة سبها ، ليبيا

الكلمات المفتاحية:

تحسين ادارة تدفق الطاقة
المركبة إلى الشبكة
مصادر الطاقات المتجددة
خوارزميات البحث

الملخص

يمكن أن تزيد عملية إدارة الطاقة من موثوقية تدفق الطاقة لتغطية الحمل في نظام الطاقة المتجددة الهجين (HRES) لا سيما في ضوء تطوير التقنيات الجديدة مثل تقنية المركبة إلى الشبكة (V2G) التي تساعد الشبكة على التعامل اثناء الذروة في تغطية الحمل. تتناول هذه الورقة نظام هجين متصل بالشبكة المستخدمة لتشغيل مبنى سكني في منطقة سبها جنوب ليبيا ، حيث يتكون من الخلايا الكهروضوئية (PV) بقدرة (112.8) كيلو وات ، و توربينات الرياح (WT) لتوليد (24) كيلوواط ، بطاريات (BT) حتى (63) كيلو وات و سيارات كهربائية (67) كيلوواط باستثمار قدره (432,513) ألف دولار. يولد النظام المقترح (2338) ميغاواط/الساعة/سنة ، وهو ما يكفي لتلبية (54.76) ٪ من الطلب على الكهرباء يتم تغطيته من مصادر الطاقة المتجددة. كما أنه يولد طاقة فائضة بقيمة (0.91) ميغاواط/ساعة/سنة ، مما يعني أن العجز في تلبية الطلب على الطاقة لا يوجد. تم تصميم النظام لتقليل التكلفة المستوية للطاقة (LCOE) وفقدان إمكانات إمداد الطاقة (LPSP) مع زيادة جزء الطاقة المتجددة (REF) من خلال تنفيذ استراتيجية تحسين إدارة الطاقة من خلال خوارزميات البحث مثل خوارزمية البحث الوقواق (CSA) و تحسين سرب الجسيمات (PSO) لتحجم مكونات النظام هجين للطاقة المتجددة ، مع

*Corresponding author:

E-mail addresses: moh.emhamed@sebhau.edu.ly, (M. Hussian) moh.abdolla@sebhau.edu.ly

, (S. Alnaghoughi) Sada.Alnaghoughi@sebhau.edu.ly

Article History : Received 31 May 2023 - Received in revised form 05 September 2023 - Accepted 02 October 2023

مراعاة البيانات المناخية و كذلك الوظائف و القيود الموضوعية. يتم تحليل توازن الطاقة بين مكونات النظام للحصول على أفضل أداء بأقل تكلفة تشغيل. تم إعداد النظام باستخدام أكواد MATLAB في تكوينات مختلفة ، وتظهر النتائج التي تم الحصول عليها قيم أداء أفضل مثل (0.0340) دولار / كيلوواط ساعة ، (0.0769)٪ ، و (0.5476)٪ ، COE ، LPSP ، و REF ، على التوالي.

1. Introduction

The inability of the electrical grid to meet the energy demand led to thinking about finding ways to support the public electricity grid, among these means is the use of renewable energies to increase the energy supply at the lowest possible cost [1].

Renewable energy technologies have become desirable, whether in connected or off-grid systems, especially after proving their reliability in energy supplies, and despite the importance of renewable energy sources in energy supplies, they are of an intermittent nature in energy generation, so these problems can be addressed by means of copying systems. Reserves such as storage batteries, Diesel Generators, and energy management systems [2], [3].

Improving the management of energy flow in Libya and in the study area is of great importance in terms of reducing the costs of energy production through the diversification of energy sources, as well as increasing the reliability of energy supply by renewable energy systems which stimulates this to address energy outages during peak energy demand, as the executive body for renewable energy in Libya has developed plans until 2030 to achieve sustainability[1], [4].

The energy flow of hybrid Photo-Voltaic systems can be managed through different optimization techniques with different energy levels. Multiple energy flow management studies have been conducted for hybrid systems to support the public grid. In reference [5] a hybrid system of Photo -Voltaic energy (PV), Wind Turbine (WT), and Diesel Generator (DG) was modeled and simulated, and this led to the possibility that renewable energy sources could be a solution for electric energy generation to replace traditional energy sources at the lowest costs.

A feasibility study for a hybrid energy system consisting of (PV / Wind / Battery) was conducted to improve the size and cost of the system components, where a computational comparison was implemented between the hybrid algorithm (Invasive Weed Optimization (IWO) - Particle Swarm Optimization (PSO)) and the evaluation of the hybrid system based on the Net Present Cost (NPC) and the Leveled Cost of Energy (LCOE). And it was shown that the hybrid algorithm (IWO-PSO) gives better results compared to other algorithms [6].

A methodology based on finding the optimal size to increase energy reliability at the lowest cost of a hybrid system (PV / WT / BT) in the grid-connected system was proposed in [7] where the study showed that this system simulation led to the effectiveness of the proposed study. Recently, in some studies, energy flow is managed by integrating electric vehicles with the grid, in addition to renewable energy sources as a hybrid system, This technology is called (V2G), in [8] put forward an integrated micro-grid system with (PV / WT / BT / EV) that aims to increase the Renewable Energy Fraction (REF), and the study showed that the proposed system can be achieved and reduce dependence on the public grid using (RESs) because of its high potential.

There are many optimization algorithms used in energy system optimization such as Particle Swarm Optimization (PSO) [9], Genetic Algorithm (GA) [10], Cuckoo search algorithm (CSA) [11], Ant Lion Optimizer

(ALO) [12], Dynamic Programming algorithm (DP) [13]. Those interested in the field of energy management are seeking to find suitable ways to integrate the grid with various renewable energy sources, including V2G technology.

The study aims to maximize the Renewable Energy Fraction (REF), minimize the Levelized Cost of Energy (LCOE), and minimize the Loss of Energy Supply Probability (LPSP), as the system operation mode is proposed in this paper by using search algorithms PSO and CSA.

The organization of the article is summarized in the introduction to the subject of the study, the mathematical modeling of the proposed system, the optimization and sizing of the system, the study methodology, the results and their discussion.

In this research, a hybrid energy system consisting of (PV / WT / BT / EV) connected to the grid was studied to cover the load of a residential building located in the city of Sebha, southwestern Libya.

2. System Model

2.1 Vehicle-to-Grid Technology

Vehicle-to-Grid (V2G) is a technology that enables electric vehicles to use their battery to send energy back to the electric grid, providing benefits to the grid. EV batteries can also be used as a mobile energy source, allowing energy to be extracted when the vehicles are not used for transmission when the Grid-to-Vehicle (G2V) mode is in place. This is particularly useful for balancing the energy demand on the grid, which can be difficult for energy plants to handle on their own [14], [15]. Figure (1) shows the block diagram of the bidirectional energy flow of EV technology to the grid.



Fig. 1: Bidirectional energy flow of V2G

2.2 The proposed grid-connected hybrid energy system

Fig. (2) shows the grid-connected hybrid energy system which consists of two buses, one of which is the Direct Current (DC) carrier connected to the wind turbines, Photo-Voltaic, and system energy storage system while the Alternating Current (AC) carrier is connected to the electric grid, electric load, and electric vehicle. The Direct and Alternating Current carriers are connected through a dual transformer to convert the current between them.

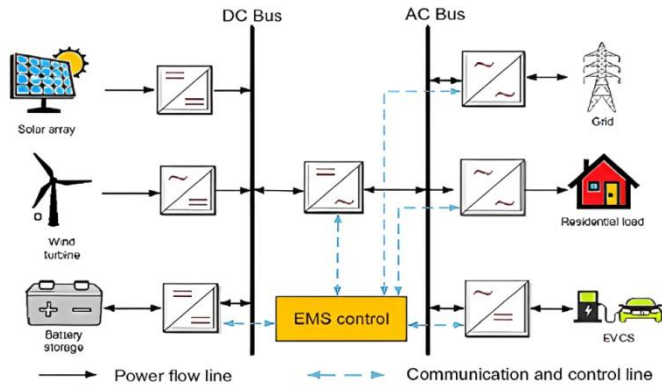


Fig. 2: Hybrid (PV / WT / BT / EV) grid-connected system

Because of the importance of managing the energy flow between the components of the system, they connect to a control unit to monitor the management of the energy flow of the entire system.

2.3 Mathematical Modelling of the system's components

The modelling process has been done using mathematical equations that help us understand and know the behaviour and interactions of the hybrid system.

Mathematical modelling of Photo-Voltaic panels can be given as:

$$P_{pv_{out}}(t) = P(pv_{rated}) * \frac{G(t)}{1000} * [1 + \alpha_t((T_{amb} + 0.0256 * G_t) - T_{c_{stc}})] \quad (1)$$

$$T_{c(stc)} = T_{amb} + G(t) * \left(\frac{NOCT-20}{800}\right) \quad (2)$$

Where:

$P_{pv_{out}}(t)$: output power generated from the PV in (W)

$G(t)$: solar irradiance in (W/m^2)

$P(pv_{rated})$: rated power for PV in (W) at standard test condition (STC)

α_t : is the temperature coefficient ($\frac{1}{^\circ C}$)

$T_{c_{stc}}$: is the cell temperature in ($^\circ C$)

T_{amb} : is the ambient temperature in ($^\circ C$)

NOCT: is the nominal operating cell temperature in ($^\circ C$) [16].

Also Mathematical modelling of Wind Turbine is represented as:

$$P_{WT} = \begin{cases} P_{WT} = 0 & v(t) \leq v_{cut_in} \\ P_r \frac{v(t) - v_{cut_in}}{v_r - v_{cut_in}} & v_{cut_in} < v_r \\ P_{WT} = P_r & v_r < v(t) < v_{cut_out} \end{cases} \quad (3)$$

Where:

v_{cut_out} : is the height known as furlong speed ($\frac{m}{s}$)

P_r : rated power speed (W)

v_r : rated wind speed ($\frac{m}{s}$)

P_{WT} : the generated output power of the WT (W)

When WT high is varying, wind speed approximated as

$$V_2 = V_1 * \left(\frac{h}{h_{ref}}\right)^\alpha \quad (4)$$

Where:

V_1, V_2 : are the wind speed ($\frac{m}{s}$)

H : is hub height (m)

h_{ref} : is the reference height anemometer (m)

α : is the power – law exponential known as wind gradient [16].

Modelling of Battery system is given in the following equations

$$C_B = \frac{E_L * AD}{DOD * \eta_{inv} * \eta_b} \quad (5)$$

$$SOC_{BT_MIN} = (1 - DOD) * C_B \quad (6)$$

$$P_b(t) = (P_{pv}(t) + P_{WT}(t)) - \frac{P_I(t)}{\eta_{inv}} \quad (7)$$

$$SOC(t) = SOC(t-1) * (1 - \sigma) + \left((P_{pv}(t) + P_{wt}(t)) - \frac{P_I(t)}{\eta_{inv}} \right) * \eta_b \quad (8)$$

$$SOC(t) = SOC(t-1) * (1 - \sigma) + \left(\frac{P_I(t)}{\eta_{inv}} - (P_{pv}(t) + P_{wt}(t)) \right) * \eta_b \quad (9)$$

$$P_{BATT}(t) = [P_I(t) - P_{wt}(t)] * \eta_{inv} - P_{pv}(t), \quad (10)$$

Where:

C_B : is the nominal capacity of the Battery (Ah)

E_L : is the daily average load demand

AD: autonomy days

DOD: is the depth of discharge (%)

η_{inv} : is the inverter efficiency (%)

η_b : is the Battery efficiency (%)

SOC: The Battery State of Charge (%)

$P_b(t)$: is the power delivered from the Battery (W)

$P_{pv}(t)$: is the total power produced from PV (W)

$P_{WT}(t)$: is the total power produced from WT (W)

$P_I(t)$: is the total energy demand (W)

σ : is the self – discharge rate of the Battery ($\frac{\%}{h}$)

SOC(t): state – of – charge of the Battery in time (t) [17].

In modelling of the electric vehicle charging station, we use the following mathematical equations as:

$$S_{rated} = \frac{K_{load} * N_{slot} * P_{EV}}{\cos \phi} \quad (11)$$

Where:

S_{rated} : is the station rated capacity (VAr)

K_{load} : is the overload factor

N_{slot} : is the amount of charging slots for each EV

P_{EV} : is the maximum power rating of each EV (KW)

$\cos \phi$: is the power factor [18].

The inverter efficiency is shown in equation (12) and mathematical equations for modelling of the grid are in equation (13) and (14).

$$P_{inv}(t) = \frac{P_I^m(t)}{\eta_{inv}}, \quad (12)$$

Where:

$P_{inv}(t)$: The inverter rating (W)

$P_I^m(t)$: the peak load demand (W)

η_{inv} : the inverter efficiency (%) [19].

$$R_{grid} = \sum_{t=1}^{8760} rate_{feed-in} * E_{grid(selling)} \quad (13)$$

$$C_{grid} = C_p * \sum_{t=1}^{8760} E_{grid(purchased)} \quad (14)$$

R_{grid} : the revenue accrued from sales of energy to the utility grid

$rate_{feed-in}$: the feed – in tariff rate ($\frac{\$}{KWh}$)

$E_{grid(selling)}$: is the selling energy price ($\$MWh$)

C_{grid} : the cost power from the grid

C_p : is the cost of buying electricity from the grid ($\frac{\$}{KWh}$)

$\sum_{t=1}^{8760} E_{grid(purchased)}$: The per hour summation of annually buying electricity from the grid for one year ($\$MWh$) [20].

3. System Size Optimization

3.1 Cost of Energy (COE)

Considering objective function aims to REF maximization while minimizing LSPS and COE. The Discounted Cash Flow (DCF) analysis method is used to calculate COE. DCF can be used to estimate the investment value based on the expected future cash flow.

COE is provided in the following Equation (15).

$$COE = \frac{(CRF * \sum_x NPC_x) + C_{grid} - R_{grid}}{E_{served} + E_{grid_selling}} \quad (15)$$

Where the Capital Recovery Factor (CRF) is given as

$$CRF = \frac{i(1+i)^n}{(1+i)^n - 1} \quad (16)$$

In equation (16) i is the real interest rate and n is the payback period/system life equal to the life of the Photo-Voltaic panel.

The Net Present Cost (NPC) (in dollars), including operating and maintenance cost, replacement cost, and present cost can be using equation (17).

$$NPC(\$) = \frac{TAC}{CRF} \quad (16)$$

TAC is Total Annual System Cost, and E_{grid_sale} means electricity sales, and in equation (15) E_{served} means primary load service in (KWh/y) [21].

3.2 Loss of Power Supply Probability (LPSP)

The reliability of the system is determined using LPSP, which is considered a second objective function to be minimized, gives as:

$$LPSP = \frac{\sum_1^{8760} P_{deficit}(t) * \Delta t}{\sum_1^{8760} P_{demand}(t) * \Delta t} \quad (17)$$

Here $P_{deficit}(t)$ is the annual power surplus and $P_{demand}(t)$ is the total load demand for the same period. In addition, values in the LPSP range $0 < LPSP < 1$, where 1 represents an unsatisfied load and 0 is a satisfied load. Also, the lowest number indicates the high reliability of the system[21].

3.3 Renewable Energy Fraction (REF)

The next objective function considered to be maximized is the REF, which is defined as the energy transferred to the load generated by RES and can be calculated as:

$$REF = \frac{\sum_1^{8760} (P_{pv} + P_{WT}) * \Delta t}{\sum_1^{8760} (P_{pv} + P_{WT} + P_{grid_purchased}) * \Delta t} \quad (18)$$

Among them, Δt represents the change over time, which is equal to 1, and $P_{grid_purchase}$ is the electricity purchased from the grid every year. Maximized REF can be minimized by the Grid Contribution Factor (GCF) given as:

$$GCF = 1 - REF \quad (19)$$

The required energy demand is met by minimizing REF[22], [23].

3.4 Constraints and Uncertainties

A. Constraints

3.4.1 The state of charge of the battery for the proposed system

In the process of charging and discharging the battery, setting limits for the State of Charge (SOC) of the battery is taken into account to extend the operational life of the battery and taking into account the operating requirements of the hybrid energy system, where the battery bank subsystem is calculated, i.e. The State of Charge SOC can be determined by constraints through the inequality in equation (21)

$$SOC_{BTmin} \leq SOC_{BT}(t) \leq SOC_{BTmax} \quad (20)$$

Where the terms SOC_{min} and SOC_{max} refer to the lowest and highest charge levels in a grid system, respectively[24].

3.4.2 Electric vehicle

Limit the exchange rate of Battery energy. The exchange rate must stay within the permitted ranges for the sake of Battery health and safety.

$$P_{Battery_min} \leq P_{Battery_batt}(t) \leq P_{Battery_max} \quad (22)$$

Where $P_{Battery}$ denotes the Battery exchange energy rate, $P_{Battery_min}$ the lowest permissible rate, and $P_{Battery_max}$ the highest permissible rate.

3.4.2.1 Limit for Battery SOC

EV Battery SOC needs to be kept within the pre-defined range to reduce Battery degeneration. Additionally, the EV Battery must be kept partially charged while keeping a specific level of energy available for EV driving, and electric vehicle constraints can be expressed as:

$$SOC_{EV_min} \leq SOC_{EV_BT}(t) \leq SOC_{EV_max} \quad (21)$$

Where SOC_{EV} is the SOC of the EV, SOC_{EV_min} is the lowest SOC that the EV is permitted to have, and SOC_{EV_max} is the highest SOC that the EV is permitted to have.

3.4.2.2 Availability of EVs

In order to provide the V2G service, EVs must be connected to the power grid; otherwise, they will not be able to use it [25].

B. Uncertainties

The change in weather conditions affects the continuity of electricity production from renewable energies due to its dependence on the climate, as the fluctuation of these renewable energies results in the difficulty of their integration with the public grid, which leads to a decrease in the efficiency of hybrid systems[26].

The characteristics of renewable energies are also affected by several factors that reduce their efficiency, for example, the thermal effect on the Photo-Voltaic module, as a result of the manufactured materials, which must be taken into account during system design.

The performance of the system is also considered one of the cases of uncertainty, and this is due to the long-term operational life of the system, as the longer the operating period, the less output and performance of the system with the same efficiency, which should be taken into account[27].

4. Methodology

The flow chart in Figure (3) shows the methodology of the study, where the data that includes climatic data, the load demand for the electric vehicle and the residential building, and the economic data of the proposed system are recalled. The Photo-Voltaic geographic information system and global solar atlas were used[28], [29], then the data were processed by MatLab software for HRES optimizing[30].

It was taken into account during the simulation that the system is a hybrid system connected to the grid and integrated with the electric vehicle, and that the system meets the energy requirements of the residential load and the electric vehicle.

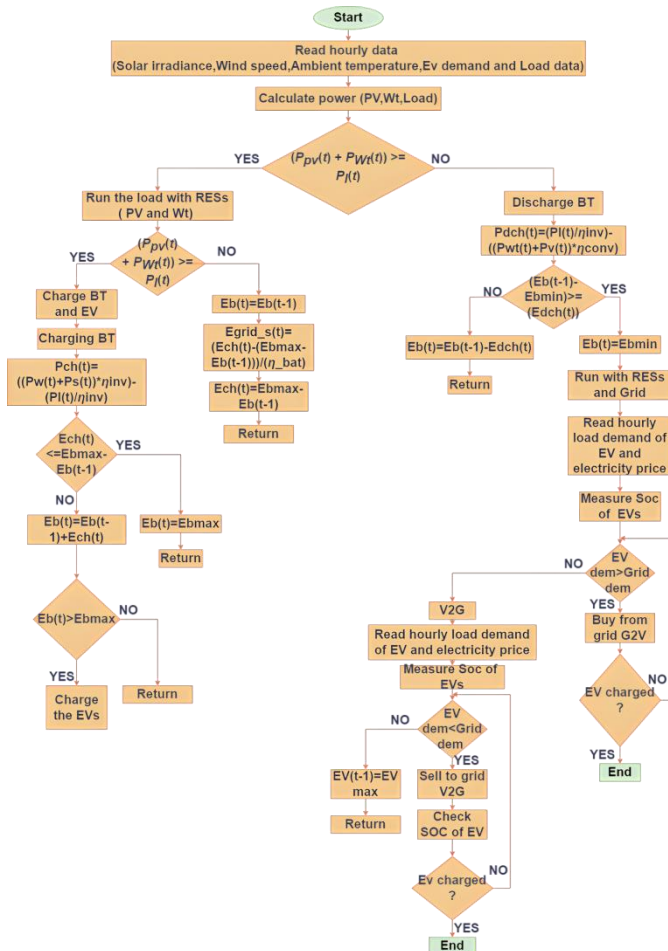


Fig. 3: Flowchart for energy flow management and optimization of a hybrid system

5. Optimization algorithms for the hybrid energy system

5.1 Particle Swarm Optimization (PSO)

PSO is a search space, includes particles where each particle is a possible solution with velocity, position, and fitness characteristics. In PSO optimization, the particle's position indicates a possible solution, while its velocity determines the direction and distance of its movement in each iteration. By updating their velocities, the particles move in the search space and get closer to the optimal solution. The quality of each particle is evaluated using a fitness function. In a standard PSO optimization process, the initial positions and initial velocities of particles are randomly assigned to create a starting swarm. The particle velocity and position i are denoted as $X_i = [x_{i1}, x_{i2}, \dots, x_{id}]$ and $V_i = [v_{i1}, v_{i2}, \dots, v_{id}]$ respectively. The update of the object and the velocity of the particle is done according to the equations as follows:

$$V_i^{k+1} = V_i^k + C1rand1(Pbest_i^k - X_i^k) + C2rand2(gbest^k - X_i^k) \tag{24}$$

$$X_i^{k+1} = X_i^k + V_i^{k+1} \tag{22}$$

The variables in this equation are represented by different parameters where: k represents the iterations, V_i^k and X_i^{k+1} represent the velocity vector, and particle position i at k -the iterations, respectively. $Pbest_i^k$ is the personal best positions for the particle i at the iteration k , $gbest^k$ is the global best vector in the entire location, $c1$, and $c2$ have acceleration coefficients of 1rand and 2rand random numbers between $[0, 1]$, [9].

5.2 Cuckoo Search Algorithm (CSA)

To simplify the explanation of the cuckoo search algorithm, three rules are used. Rule one each cuckoo lays one egg at a time and tosses it randomly into a nest. Then rule two the best nests with high-quality eggs are passed on to the next generation. Rule three the number of available host nests is fixed, and the host may detect alien eggs with probability Pa $[0, 1]$. In this situation, the host bird can either dispose of the egg or leave the nest and construct a fresh one at a new location. To make things simpler, let's say that a fraction Pa of n nests is replaced with new ones (containing random solutions at newer positions). In terms of maximizing performance, the fitness or quality of a solution is directly proportional to the objective function. Similarly, other kinds of fitness can be determined by utilizing the fitness function in GA. So, in summary, the fundamental steps of cuckoo search algorithms can be described as follows in pseudo-code. When creating a new solution, $X^{(t+1)}$, for example, cuckoo i , a Lévy flight is performed as:

$$x_i^{t+1} = x_i^t + \alpha \oplus Lévy(\lambda), \tag{23}$$

The step size α is related to the scales of the problem, so it should have a positive value. In the majority of cases, we can expect α to be $O(1)$. The product \oplus is an acronym that means multiplying items one at a time. Lévy flight is essentially a random walk, but their random steps are drawn from a Lévy distribution for large steps, which has an infinite variance and infinite mean as

$$Lévy \sim u = t^{-\lambda}, (1 < \lambda < 3) \tag{24}$$

Here, the sequential jumps of a cuckoo essentially resemble a random walk that follows a energy-law step-length distribution with a long tail[11].

Figure (4) shows the use of the proposed approach for the (CSA) and (PSO) algorithms in the following flowchart along with setting the parameters to achieve the objective functions (REF), (LPSP) and (LCOE). The planned objective functions were accomplished because the study area is privileged to experience a variety of weather conditions.

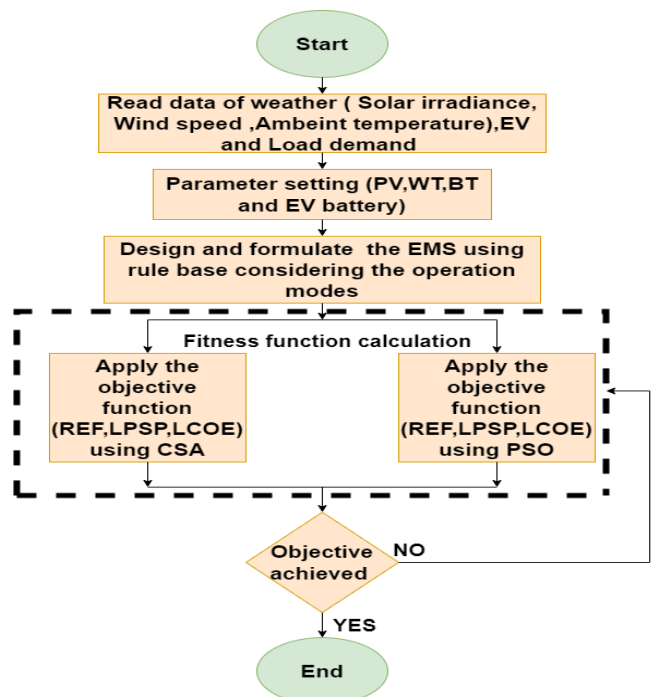


Fig. 4: Flowchart of the objective function while using the operating parameters of the proposed method.

6. Results and discussion
6.1 Total Load demand

The electrical load can be estimated to know the amount of energy required, as it varies seasonally throughout the year. Fig. (5) shows the daily consumed load for the seasons of the year for a residential building in the city of Sebha for the current year. We note that the highest electrical load is in the summer and then winter due to the operation of heating and cooling devices. The peak load is at noon and the lowest load is after sunset. As for the fall and spring seasons, they are the least consuming load during the year due to the mild climate and the lack of use of devices that consume a high load. Figures (6), (7) and (8) also show weather data hours in terms of temperature, solar radiation and wind speed for one year, respectively.

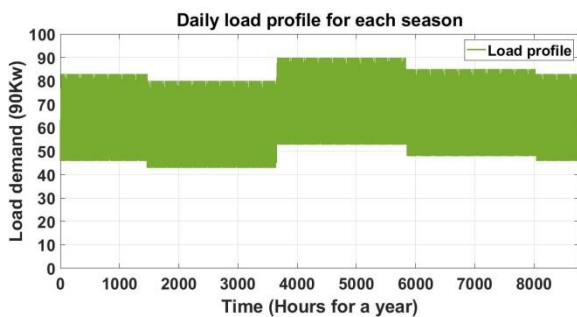


Fig. 5: Residential load file hours for a year

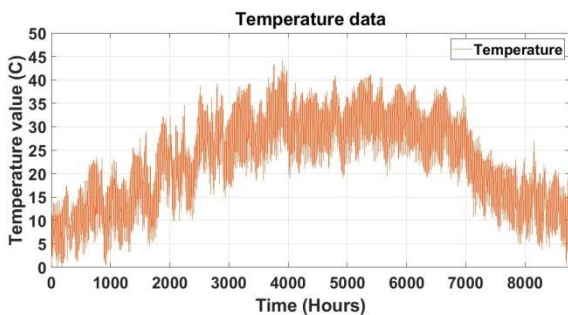


Fig. 6: Annual temperature data for a year

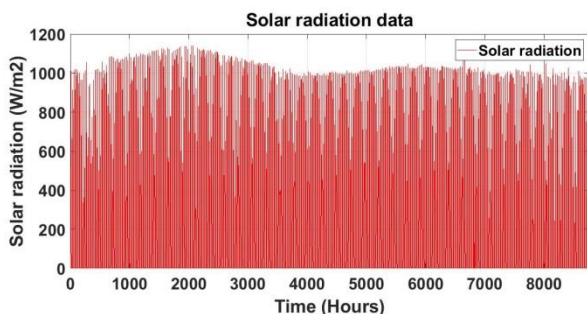


Fig. 7: Annual solar radiation data for one year

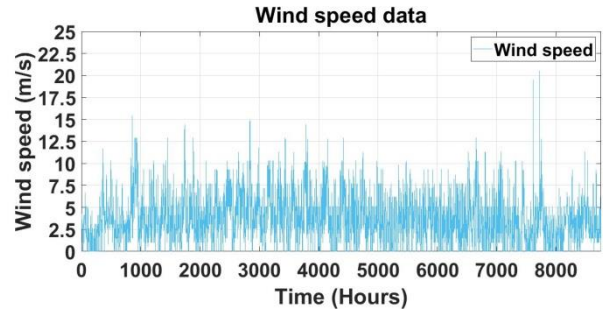


Fig. 8: Annual wind speed data for a year

Also as shown in figure (9) the daily electric vehicle load demand, which assumed to be constant. The total load can be computed from the residential building consumption combined with the electrical vehicle's load.

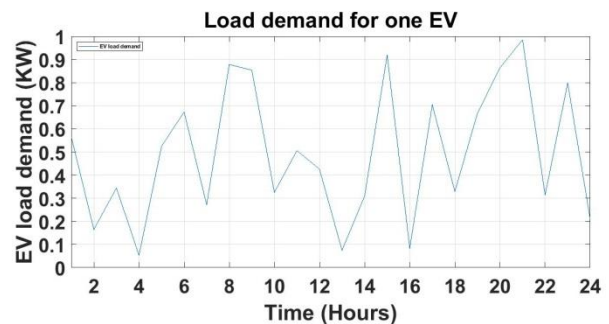


Fig. 9: Daily load demand of the electric vehicle

6.2 System Component Specifications

Knowing the specifications of the components of the system is important because it enters into giving all the necessary data on the basis of which the energy management in the system is improved and analyzed after preparing the mathematical formula for each component. Table1 shows the proposed specifications.

Table 1: Technical Specifications of the system[31].

Component name	Component type	Capacity	Capital cost
PV system	KD325GX-LFB	325W	1200 \$
Wind turbine	Eo cycle	5 kW	2300 \$
Battery system	deep cycle(LiFePO4)	40 kWh	167 \$
Inverter	Dual	115kw	127 \$
Electrical grid	Power price (sell)	0.05 \$/Kwh	-
		0.04 \$/Kwh	-
Electrical load	household building	90kw	-
Electrical vehicle	Lithium-Ion	14.1 kWh	8097 \$

6.3 System Performance

The study relied on CSA and PSO algorithms to design a grid-connected system consisting of (PV / WT / BT / EV) as shown in Fig. (2). The proposed system in the study area of the Sabha region in Libya to cover the total load in section 6.1. The proposed system is designed to take advantage of RESs and V2G technology in energy

exchange and assist the public grid in covering the electric load, taking into account the climate data of the study area and the mathematical modeling of the system components in addition to the objective functions and constraints.

6.3.1 V2G Energy exchange

Figure (10) shows the balance of energy flow, where the black, green, red, blue and purple colors represent the load, the purchase of energy from the grid, the energy generated from the battery, the wind energy and the photo-voltaic energy respectively, Which is managed through BT and V2G. The positive impact on load coverage can be seen in terms of the state of charge and discharge of batteries SOC% for one week in a year. The study also takes into account the importance of V2G technology in Figures (11) and (12), which represent the exchange of energy between the electric vehicle and the grid, and vice versa, the charging state of electric vehicles. Used in the system for (10) electric vehicles as a reliable energy source to increase the reliability of energy supplies in the absence of RESs and batteries in the system.

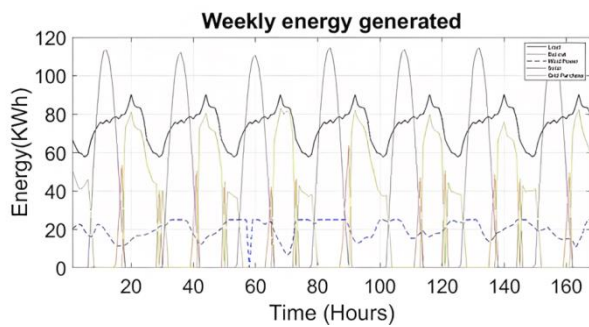


Fig. 10: Energy flow between the components of the proposed system

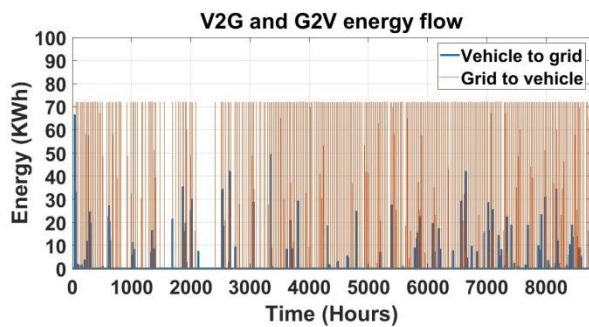


Fig. 11: Energy exchange between the electric vehicle and the grid

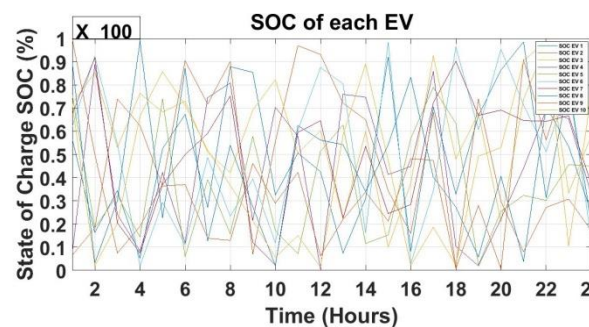


Fig. 12: charging status of electric vehicles

6.3.2 Optimum size of proposed System

Simulation is implemented in MATLAB codes for PSO and CSA optimization. The optimal system configuration obtained is depicted in Table 2. Note that the results obtained based on CSA and PSO are approximately same each other, the obtained results show better performance values such as (0.0340) \$/KWh, (0.0769) %, and (0.5476) % for COE, LPSP, and REF, respectively. Additionally, the optimum size values such as (350), (5), and (4) for PV modules, WTs, and BTs.

Table 2: Optimum size of proposed System.

Parameters	CSA	PSO
COE(\$/KWh)	0.0340	0.0347
LPSP(%)	0.0769	0.0770
REF(%)	0.5476	0.5475
GCF(%)	0.4524	0.4525
NPC	2.5766*e5	2.5768*e5
ASC(\$/y)	2.2464e4	2.2466e4
AD	3	2
Npv	350	350
Nwt	5	5
Nbt	5	4

Table 3: The results of the energy generated for an optimal size system.

Generated and Consumption energy (MWh/year)	
Photo-Voltaic	988.783
Wind turbine	210.379
Battery of system	552.246
Electric vehicle	587.309
Total	2338.807
Electrical grid load	788.923
Electrical vehicle load	631.138
Total	1420.061
Surplus energy	918.656
Deficit energy	-

6.3.3 Convergence of CSA & PSO algorithms

The results showed that the CSA can perform faster than the PSO to obtain the best sizing of the components of the system with minimum cost, as shown in Figure (13), and the convergence for CSA is better than the PSO, where the first algorithm converged in 3 iterations and the second at 5 iterations approximately.

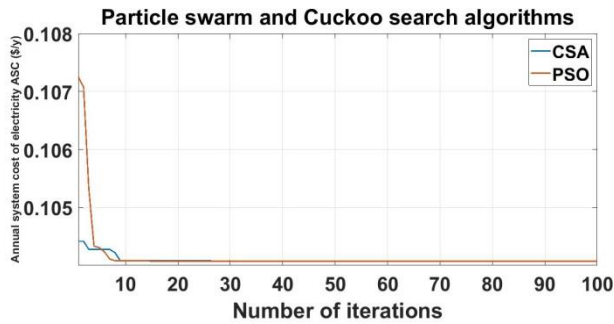


Fig. 13: Convergence of CSA&PSO algorithms

7. Conclusion

The study demonstrates the effectiveness of incorporating V2G into a system configuration that uses PV-WT-BT with AC residential load plus EV load and the system is connected to the grid system by selecting the optimal size of the system, improving its performance, and reducing losses and costs while increasing reliance on energy sources, as well as the use of algorithms inspired by nature, such as CSA and PSO, and comparing the results between them. The study also takes into account weather data and seasonal changes to improve system performance. The proposed system performs better compared to the measurement test using three test functions, and the study site has high energy production capabilities with the RES used. Therefore, the proposed system could be a viable solution to reduce dependence on the main grid and increase the use of renewable energy sources.

References

- [1]- A. Guwaeder and R. Ramakumar, "A Study of Grid-connected Photovoltaics in the Libyan Power System," *Energy and Power*, vol. 7, no. 2, pp. 41–49, 2017, doi: 10.5923/j.ep.20170702.02.
- [2]- M. A. Yazdanpanah-Jahromi, S. M. Barakati, and S. Farahat, "An efficient sizing method with suitable energy management strategy for hybrid renewable energy systems," *Int. Trans. Electr. Energy Syst.*, vol. 24, no. 10, pp. 1473–1492, 2014, doi: 10.1002/etep.1790.
- [3]- J. Singh, M. Kumar, A. Sharma, G. Pandey, K. Chae, and S. Lee, "We are IntechOpen, the world's leading publisher of Open Access books Built by scientists, for scientists TOP 1%," *Intech*, vol. 11, no. tourism, p. 13, 2016, [Online]. Available: <https://www.intechopen.com/books/advanced-biometric-technologies/liveness-detection-in-biometrics>
- [4]- S. Makken, "A Comprehensive Economic Analysis of Solar and Wind Power and its Suitability A Comprehensive Economic Analysis of Solar and Wind Power and its Suitability to Libya," no. September, 2022.
- [5]- Q. Hassan, M. Jaszczur, and J. Abdulateef, "Optimization of PV/WIND/DIESEL Hybrid Power System in HOMER for Rural Electrification," *J. Phys. Conf. Ser.*, vol. 745, no. 3, 2016, doi: 10.1088/1742-6596/745/3/032006.
- [6]- M. Kharrich, M. Akherraz, and Y. Sayouti, "Optimal sizing and cost of a Microgrid based in PV, WIND and BESS for a School of Engineering," *2017 Int. Conf. Wirel. Technol. Embed. Intell. Syst. WITS 2017*, 2017, doi: 10.1109/WITS.2017.7934648.
- [7]- U. Akram, M. Khalid, and S. Shafiq, "Optimizing a grid-connected micro-grid with optimal renewable generation and battery energy storage," *2017 9th IEEE-GCC Conf. Exh. GCCCE 2017*, pp. 1–9, 2018, doi: 10.1109/IEEGGCC.2017.8448232.
- [8]- O. D. T. Odou, R. Bhandari, and R. Adamou, "Hybrid off-grid renewable power system for sustainable rural electrification in Benin," *Renew. Energy*, vol. 145, pp. 1266–1279, 2020, doi: 10.1016/j.renene.2019.06.032.
- [9]- R. R. Nivedha, J. G. Singh, and W. Ongsakul, "PSO based economic dispatch of a hybrid microgrid system," *EPSCICON 2018 - 4th Int. Conf. Power, Signals, Control Comput.*, pp. 1–5, 2018, doi: 10.1109/EPSCICON.2018.8379595.
- [10]- M. S. Ismail, M. Moghavvemi, and T. M. I. Mahlia, "Genetic algorithm based optimization on modeling and design of hybrid renewable energy systems," *Energy Convers. Manag.*, vol. 85, pp. 120–130, 2014, doi: 10.1016/j.enconman.2014.05.064.
- [11]- S. Berrazouane and K. Mohammedi, "Parameter optimization via cuckoo optimization algorithm of fuzzy controller for energy management of a hybrid power system," *Energy Convers. Manag.*, vol. 78, pp. 652–660, 2014, doi: 10.1016/j.enconman.2013.11.018.
- [12]- S. Mirjalili, "The ant lion optimizer," *Adv. Eng. Softw.*, vol. 83, pp. 80–98, 2015, doi: 10.1016/j.advengsoft.2015.01.010.
- [13]- L. An and T. Tuan, "Dynamic Programming for Optimal Energy Management of Hybrid Wind-PV-Diesel-Battery," *Energies*, vol. 11, no. 11, p. 3039, 2018, doi: 10.3390/en11113039.
- [14]- B. Vani, D. Chaturvedi, and P. Yadav, "Grid Management through Vehicle-To-Grid Technology," *Int. J. Recent Technol. Eng.*, vol. 10, no. 2, pp. 5–9, 2021, doi: 10.35940/ijrte.b6036.0710221.
- [15]- K. Kasturi, "Electric vehicles management enabling G2V and V2G in smart distribution system for maximizing profits using MOMVO," no. December 2018, pp. 1–17, 2019, doi: 10.1002/2050-7038.12013.
- [16]- A. L. Bakar, C. W. Tan, and K. Y. Lau, "Optimal sizing of an autonomous photovoltaic/wind/battery/diesel generator microgrid using grasshopper optimization algorithm," *Sol. Energy*, vol. 188, no. March, pp. 685–696, 2019, doi: 10.1016/j.solener.2019.06.050.
- [17]- M. Kharrich, Y. Sayouti, and M. Akherraz, "Microgrid sizing with environmental and economic optimization," *3rd Renew. Energies, Power Syst. Green Incl. Econ. REPS GIE 2018*, vol. 2, no. 2, pp. 1–6, 2018, doi: 10.1109/REPSGIE.2018.8488864.
- [18]- A. Arancibia and K. Strunz, "Modeling of an electric vehicle charging station for fast DC charging," *2012 IEEE Int. Electr. Veh. Conf. IEVC 2012*, no. 3, 2012, doi: 10.1109/IEVC.2012.6183232.
- [19]- S. Singh, M. Singh, and S. C. Kaushik, "Feasibility study of an islanded microgrid in rural area consisting of PV, wind, biomass and battery energy storage system," *Energy Convers. Manag.*, vol. 128, pp. 178–190, 2016, doi: 10.1016/j.enconman.2016.09.046.
- [20]- S. Barakat, H. Ibrahim, and A. A. Elbaset, "Multi-objective optimization of grid-connected PV-wind hybrid system considering reliability, cost, and environmental aspects," *Sustain. Cities Soc.*, vol. 60, no. March, p. 102178, 2020, doi: 10.1016/j.scs.2020.102178.
- [21]- M. M. Samy, M. I. Mosaad, M. F. El-Naggar, and S. Barakat, "Reliability Support of Undependable Grid Using Green Energy Systems: Economic Study," *IEEE Access*, vol. 9, pp. 14528–14539, 2021, doi: 10.1109/ACCESS.2020.3048487.
- [22]- A. Hiendro, I. Yusuf, F. T. Pontia Wigiyanto, K. Hie Khwee, and J. Junaidi, "Optimum Renewable Fraction for Grid-connected Photovoltaic in Office Building Energy Systems in Indonesia," *Int. J. Power Electron. Drive Syst.*, vol. 9, no. 4, p. 1866, 2018, doi: 10.11591/ijpeds.v9.i4.pp1866-1874.
- [23]- A. M. Jasim, B. H. Jasim, F. C. Baiceanu, and B. C. Neagu, "Optimized Sizing of Energy Management System for Off-Grid Hybrid Solar/Wind/Battery/Biogasifier/Diesel Microgrid System," *Mathematics*, vol. 11, no. 5, 2023, doi: 10.3390/math11051248.
- [24]- N. Attou, S. A. Zidi, M. Khatir, and S. Hadjeri, "Energy management system for hybrid microgrids," *EEA - Electroteh. Electron. Autom.*, vol. 69, no. 2, pp. 21–30, 2021, doi: 10.46904/EEA.21.69.2.1108003.
- [25]- K. Miao, V. K. Ramachandaramurthy, and J. Y. Yong, "Integration of electric vehicles in smart grid: A review on vehicle to grid technologies and optimization techniques,"

- Renew. Sustain. Energy Rev.*, vol. 53, pp. 720–732, 2016, doi: 10.1016/j.rser.2015.09.012.
- [26]- D. Maradin, “Advantages and disadvantages of renewable energy sources utilization,” *Int. J. Energy Econ. Policy*, vol. 11, no. 3, pp. 176–183, 2021, doi: 10.32479/ijeep.11027.
- [27]- Y. F. Nassar *et al.*, “Design of an isolated renewable hybrid energy system: a case study,” *Mater. Renew. Sustain. Energy*, vol. 11, no. 3, pp. 225–240, 2022, doi: 10.1007/s40243-022-00216-1.
- [28]- “6e0f20ca10e754909b5ecce2a3e83209ef36b504 @ re.jrc.ec.europa.eu.” [Online]. Available: https://re.jrc.ec.europa.eu/pvg_tools/en/
- [29]- solargis, “Map @ Globalsolaratlas.Info,” *Global Solar Atlas*. 2020. [Online]. Available: <https://globalsolaratlas.info/map?c=8.431621,-11.060486,8&r=SLE&s=7.885936,-11.18639&m=site>
- [30]- Mathworks, “MATLAB @ www.mathworks.com.” 2016. [Online]. Available: <http://www.mathworks.com/products/matlab/>
- [31]- A. Alsharif, C. W. Tan, R. Ayop, K. Y. Lau, and A. M. d. Dobi, “A rule-based power management strategy for Vehicle-to-Grid system using antlion sizing optimization,” *J. Energy Storage*, vol. 41, no. April, p. 102913, 2021, doi: 10.1016/j.est.2021.102913.